

Fang-Howard wave function modelling of electron mobility in AlInGaN/AlN/InGaN/GaN double heterostructures

Yao Li(李姚) and Hong-Bin Pu(蒲红斌)

Citation: Chin. Phys. B, 2021, 30 (**9**): 097201. DOI: 10.1088/1674-1056/abea87
Journal homepage: http://cpb.iphy.ac.cn; http://iopscience.iop.org/cpb

What follows is a list of articles you may be interested in

Effect of overdrive voltage on PBTI trapping behavior in GaN MIS-HEMT with LPCVD SiN_x gate dielectric

Tao-Tao Que(阙陶陶), Ya-Wen Zhao(赵亚文), Liu-An Li(李柳暗), Liang He(何亮), Qiu-Ling Qiu(丘秋凌), Zhen-Xing Liu(刘振兴), Jin-Wei Zhang(张津玮), Jia Chen(陈佳), Zhi-Sheng Wu(吴志盛), Yang Liu(刘扬)
Chin. Phys. B, 2020, 29 (**3**): 037201. DOI: 10.1088/1674-1056/ab696b

Temperature dependence on the electrical and physical performance of InAs/AlSb heterojunction and high electron mobility transistors

Jing Zhang(张静), Hongliang Lv(吕红亮), Haiqiao Ni(倪海桥), Zhichuan Niu(牛智川), Yuming Zhang(张玉明)
Chin. Phys. B, 2018, 27 (**9**): 097201. DOI: 10.1088/1674-1056/27/9/097201

Effect of depositing PCBM on perovskite-based metal-oxide-semiconductor field effect transistors

Su-Zhen Luan(栾苏珍), Yu-Cheng Wang(汪钰成), Yin-Tao Liu(刘银涛), Ren-Xu Jia(贾仁需)
Chin. Phys. B, 2018, 27 (**4**): 047208. DOI: 10.1088/1674-1056/27/4/047208

Low-temperature physical properties and electronic structures of Ni_3Sb, Ni_5Sb_2, $NiSb_2$, and NiSb

Luo Xiao-Ning, Dong Cheng, Liu Shi-Kai, Zhang Zi-Ping, Li Ao-Lei, Yang Li-Hong, Li Xiao-Chuan
Chin. Phys. B, 2015, 24 (**6**): 067201. DOI: 10.1088/1674-1056/24/6/067201

Localization correction to the anomalous Hall effect in amorphous CoFeB thin films

Ding Jin-Jun, Wu Shao-Bing, Yang Xiao-Fei, Zhu Tao
Chin. Phys. B, 2015, 24 (**2**): 027201. DOI: 10.1088/1674-1056/24/2/027201

Fang–Howard wave function modelling of electron mobility in AlInGaN/AlN/InGaN/GaN double heterostructures*

Yao Li(李姚)[1,2,3,†] and Hong-Bin Pu(蒲红斌)[1,3]

[1] Department of Electronic Engineering, Xi'an University of Technology, Xi'an 710048, China
[2] Key Laboratory of Wide Bandgap Semiconductor Materials, Ministry of Education, Xi'an 710071, China
[3] Xi'an Key Laboratory of Power Electronic Devices and High Efficiency Power Conversion, Xi'an 710048, China

(Received 27 November 2020; revised manuscript received 21 January 2021; accepted manuscript online 1 March 2021)

To study the electron transport properties in InGaN channel-based heterostructures, a revised Fang–Howard wave function is proposed by combining the effect of GaN back barrier. Various scattering mechanisms, such as dislocation impurity (DIS) scattering, polar optical phonon (POP) scattering, piezoelectric field (PE) scattering, interface roughness (IFR) scattering, deformation potential (DP) scattering, alloy disorder (ADO) scattering from InGaN channel layer, and temperature-dependent energy bandgaps are considered in the calculation model. A contrast of AlInGaN/AlN/InGaN/GaN double heterostructure (DH) to the theoretical AlInGaN/AlN/InGaN single heterostructure (SH) is made and analyzed with a full range of barrier alloy composition. The effect of channel alloy composition on InGaN channel-based DH with technologically important Al(In,Ga)N barrier is estimated and optimal indium mole fraction is 0.04 for higher mobility in DH with $Al_{0.4}In_{0.07}Ga_{0.53}N$ barrier. Finally, the temperature-dependent two-dimensional electron gas (2DEG) density and mobility in InGaN channel-based DH with $Al_{0.83}In_{0.13}Ga_{0.04}N$ and $Al_{0.4}In_{0.07}Ga_{0.53}N$ barrier are investigated. Our results are expected to conduce to the practical application of InGaN channel-based heterostructures.

Keywords: scattering mechanism, double heterostructures, electron mobility, InGaN channel

PACS: 72.20.Fr, 72.80.Cw, 72.20.Dp **DOI:** 10.1088/1674-1056/abea87

1. Introduction

InGaN material has proved its potential for the realization of blue-green light-emitting diodes and laser diodes.[1] Owing to the large carrier sheet density attainable and relatively high saturation velocity, the heterojunction field effect transistors (HFETs) using InGaN alloys as channels layer promise in high-frequency and large-power fields. Furthermore, the relatively small bandgap of InGaN materials conduces to enlarging the discontinuity of conduction band and leads to better carrier confinement in the quantum well. However, the growth of InGaN layer is still a challenge due to the solid phase immiscibility of InN and GaN and the interdiffusion of In and Ga in InGaN/GaN system.[2] The randomly distributed In and Ga atoms at the periodic lattice sites also cause ADO scattering, which is proved to be one of the main issues limiting the carrier mobility of InGaN channel heterostructures.[3,4] Therefore, further optimizations of the heterostructure and process are necessary to fully realize the potential of InGaN channel HFETs.

The insertion of a thin AlN interlayer between AlInN barrier and GaN channel contributes to the increase of conduction band offset and the elimination of the ADO scattering from barrier layer, which results in higher two-dimensional electron gas (2DEG) density and electron mobility[5,6] Zhang *et al.*[7] adopted a two-step AlN interlayer in AlGaN/InGaN heterostructure and improved the channel electron mobility to 1681 $cm^2/V{\cdot}s$ due to the relatively smooth interface between barrier and buffer layer. Laboutin *et al.*[8] realized the record electron mobilities from 1070 $cm^2/V{\cdot}s$ to 1290 $cm^2/V{\cdot}s$ with a sheet carrier density of $\sim 2\times10^{13} cm^{-2}$ in AlInGaN/AlN/$In_xGa_{1-x}N$ (x = 0.05–0.1) high electron mobility transistor (HEMT) structures. Wang *et al.*[9] designed a depletion-mode HEMT with $In_{0.13}Al_{0.83}Ga_{0.04}N$/AlN/$In_{0.05}Ga_{0.95}N$ heterojunction on an SiC substrate and obtained a record high $\sqrt{f_T \cdot f_{max}}$ of 239 GHz. Xie *et al.*[10] declared an improved mobility of 1230 cm^{-2} for indium-doped AlGaN barrier with $In_{0.04}Ga_{0.96}N$ channel. Recently, we studied the electron mobility in AlInGaN/InGaN heterostructures and analyzed in detail the scattering mechanisms,[11] while the practically grown InGaN channel layer is generally few nanometers thick and is achieved on a thick GaN buffer layer, which significantly changes the distribution and density of 2DEG in the channel. In this work, the electronic transport properties in AlInGaN/AlN/InGaN/GaN double heterostructure (DH) are recalculated based on a modified Fang–Howard (FH) wave function[12] and analyzed as a function of alloy composition and temperature.

*Project supported by the Xi'an Science and Technology Program, China (Grant No. 2019217814GXRC014CG015-GXYD14.3) and the Open Project of Key Laboratory of Wide Band-gap Semiconductor Materials, Ministry of Education, China (Grant No. Kdxkf2019-01).

†Corresponding author. E-mail: liyao@xaut.edu.cn

© 2021 Chinese Physical Society and IOP Publishing Ltd

2. Results and discussion

In AlInGaN/AlN/InGaN/GaN DH as shown in Fig. 1, electron confinement in the channel is modified and a DH-based Fang–Howard model is proposed to calculated the electron distribution.[12] That is, a new form of 2DEG wave function $u(z)$ is established with considering the joint polarization effects from the top AlInGaN/InGaN and bottom InGaN/GaN heterostructures and $u(z)$ equals $Nz\left(\mathrm{e}^{-bz/2}-\mathrm{e}^{-bt/2}\right)$ for $0<z<t$, where t is the thickness of InGaN channel and parameters N and b are resolved from normalization condition $\int_0^t |u(z)|^2 \mathrm{d}z = 1$, otherwise, $u(z)$ vanishes. Accordingly, 2DEG density can be computed by applying Gauss' law at each heterointerface. In terms of the scattering process, we consider the DP scattering, PE scattering, POP scattering, DIS scattering, IFR scattering, and ADO scattering. Based on the models in SH, the relaxation time for each scattering mechanism is analytically computed by using a mathematical software with two renewed form factors: $F(q) = \int u^2(z)\,\mathrm{e}^{-qz}\mathrm{d}z$, and $G(q) = \int \mathrm{d}z_1\,\mathrm{d}z_2 u^2(z_1)\,u^2(z_2)\exp(-q|z_1-z_2|)$ regarding to the DH-based 2DEG wave function. Owing to the introduction of AlN interlayer, barrier ADO scattering is eliminated and the electrons suffer only the channel ADO scattering. The calculations are similar to those in Ref. [11]. The thicknesses of the barrier and channel layers are assumed to be 17 nm and 12 nm[10,13] unless otherwise stated. The parameters of correlation length and RMS roughness are taken as 2.5 nm[3] and 0.45 nm,[10,13] respectively. The dislocation density is set to be 1.3×10^9 cm^{-2} and the metal work function is assumed to be 5.1 eV for Au gate contact.[14] The rest parameters involved in the calculation are taken from Ref. [15].

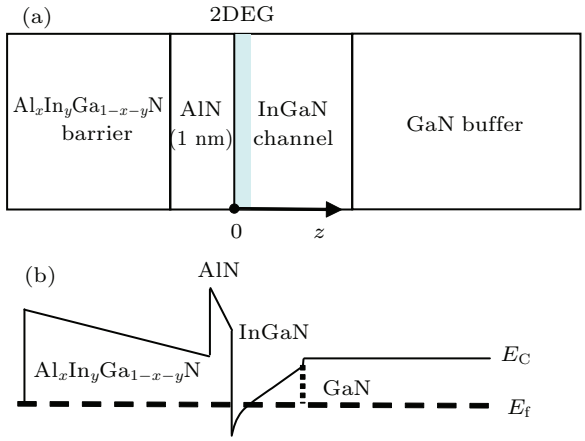


Fig. 1. Schematic diagram of calculated AlInGaN/AlN/InGaN/GaN DH, showing (a) epitaxy structure and (b) conduction band profile.

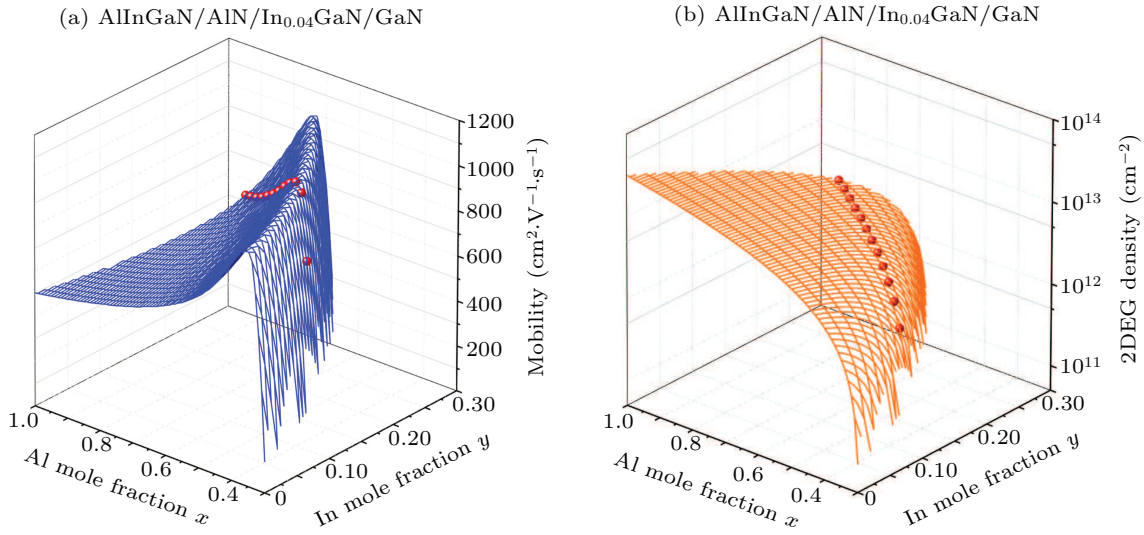


Fig. 2. Electronic transport properties in AlInGaN/AlN/$In_{0.04}$GaN/GaN DH at room temperature, with red balls denoting LM DH.

We first compare the electronic transport properties in AlInGaN/AlN/$In_{0.04}$GaN with and without GaN back barrier layer, whose variations with barrier alloy composition are displayed in Figs. 2 and 3. Thereinto, the lattice-matched (LM) heterostructures are indicated in red balls with indium mole fraction y relating to aluminum mole fraction x in AlInGaN barrier as $y = 0.224x + 0.04$. As shown, both electron mobility and 2DEG density surface in AlInGaN/AlN/$In_{0.04}$GaN/GaN DH and AlInGaN/AlN/$In_{0.04}$GaN SH are similar, the former presents parabolic curves along the directions of increasing aluminum content and indium content, while 2DEG density is apparently proportional to aluminum composition and inversely proportional to indium composition of AlInGaN barrier. The scope of barrier alloy composition in AlInGaN/AlN/$In_{0.04}$GaN/GaN DH is narrowed due to the superimposed electric field caused by the polarization charges at the bottom InGaN/GaN interface.[12] For clarity, we extract the theoretical data for LM heterojunction from Figs. 2 and 3, and contrast the effects of detailed scattering mechanisms in Fig. 4. As indicated in Fig. 4, the 2DEG density increases with increasing aluminum mole fraction in AlInGaN barrier due to the enlarged conduction band offset and po-

larization charges at AlInGaN/AlN/$In_{0.04}$GaN heterointerface, whose value is lower in InGaN channel-based DH than that in SH caused by the effect of GaN back barrier. For the InGaN channel-based SH in Fig. 4(a), the effects of ADO scattering and PO scattering are almost equally important in the whole range of alloy composition, while the effect of DIS scattering fades away due to the strengthened screening effect by relatively large two-dimensional electron gas density. For InGaN channel-based DH in Fig. 4(b), the mobility curve is mainly determined by DIS scattering for lower two-dimensional electron gas density and ADO scattering for relatively high electron density.

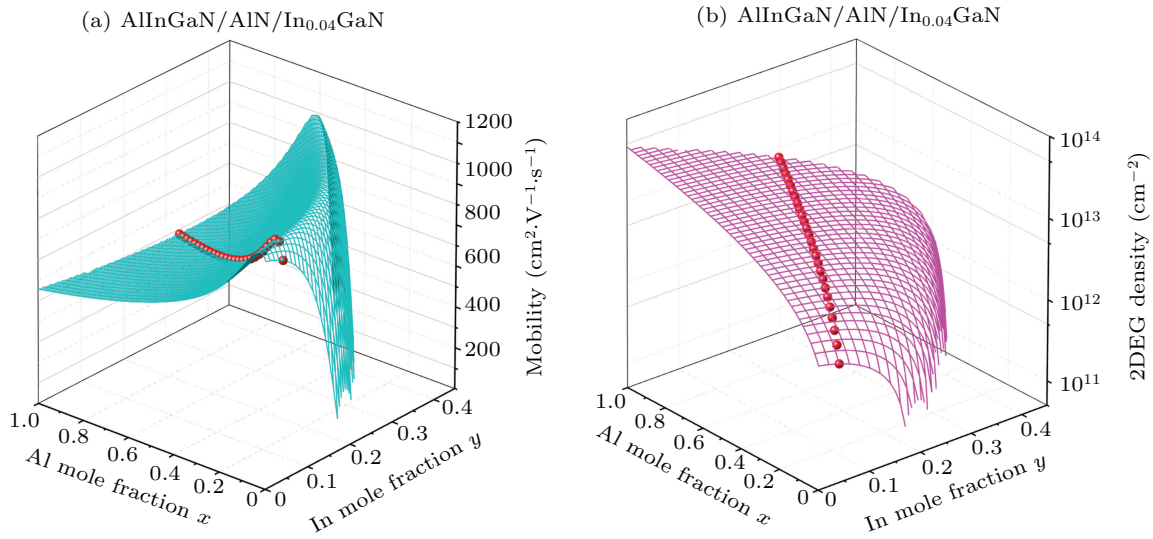


Fig. 3. Electronic transport properties in AlInGaN/AlN/$In_{0.04}$GaN SH at room temperature, with red balls denoting LM SH.

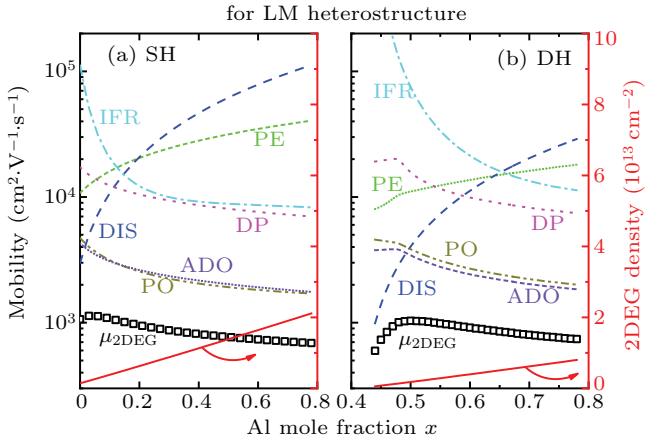


Fig. 4. The mobility limited by various scattering mechanisms in LM AlInGaN/AlN/$In_{0.04}$GaN SH and AlInGaN/AlN/$In_{0.04}$GaN/GaN DH at room temperature.

Then the electronic transport property in AlInGaN/AlN/InGaN/GaN DH is analyzed as a function of indium mole fraction in InGaN channel layer. Since the technologically important AlInGaN barrier layers are either indium-doped AlGaN or gallium-doped AlInN, the comparisons in 2DEG mobility and density among InGaN channel heterostructures with $Al_{0.4}In_{0.07}Ga_{0.53}N$, $Al_{0.4}Ga_{0.6}N$, $Al_{0.83}In_{0.13}Ga_{0.04}N$, and $Al_{0.83}In_{0.17}N$ barriers are conducted. The results are shown in Fig. 5. As shown in the figure, with the increase of indium mole fraction in InGaN channel, the mobility in AlInGaN/AlN/InGaN/GaN DH with $Al_{0.4}In_{0.07}Ga_{0.53}N$ barrier first increases for indium content less than 0.04 and then gradually decreases, while the curves for DH with other barriers decline uniformly. The detailed mechanisms are discussed below. In contrast with the mobility value in InGaN channel-based DH with $Al_{0.4}Ga_{0.6}N$ barrier, replacing few gallium by indium in barrier layer reduces the mobility for InGaN channel with relatively small indium content (less than 0.35), but increases the mobility hereafter. While for AlInN-like barrier layer, the substitution of indium for gallium brings a minor effect on electron mobility. As shown in Fig. 5(b), 2DEG density increases after indium has been substituted for gallium with aluminum mole fraction fixed in Al(In)GaN barriers, which is due to the enhancing polarization strength at Al(In)GaN/InGaN heterointerface.

To illustrate the effects of different barrier layers, the variations of mobility limitedby various scattering mechanisms in AlInGaN/AlN/InGaN/GaN DH are computed and the results are shown in Fig. 6. Here, $Al_{0.4}In_{0.07}Ga_{0.53}N$ and $Al_{0.83}In_{0.13}Ga_{0.04}N$ barriers are taken for example. As shown in Fig. 6(a), when indium content in InGaN channel is small, the 2DEG mobility in $Al_{0.4}In_{0.07}Ga_{0.53}N$/AlN/InGaN/GaN DH is determined mainly by DIS scattering. With indium composition increasing further, ADO scattering becomes strong and dominates the 2DEG mobility. Therefore, the calculated 2DEG mobility first increases to a maximum value at indium mole fraction of 0.04 in InGaN channel and then descends with indium content increasing. Since the increased 2DEG density in InGaN channel-based DH with $Al_{0.4}Ga_{0.6}N$

depresses DIS scattering and highlights the effect of ADO scattering, the final 2DEG mobility decreases directly and turns lower than that for the case with $Al_{0.4}In_{0.07}Ga_{0.53}N$ barrier. For DH with $Al_{0.83}In_{0.13}Ga_{0.04}N$ barrier, as displayed in Fig. 6(b), the 2DEG mobility is mainly determined by POP and ADO scatterings and decreases monotonically with the increase of indium composition in InGaN channel. For this case, electron mobility is immune to the substitution of little gallium for indium in barrier.

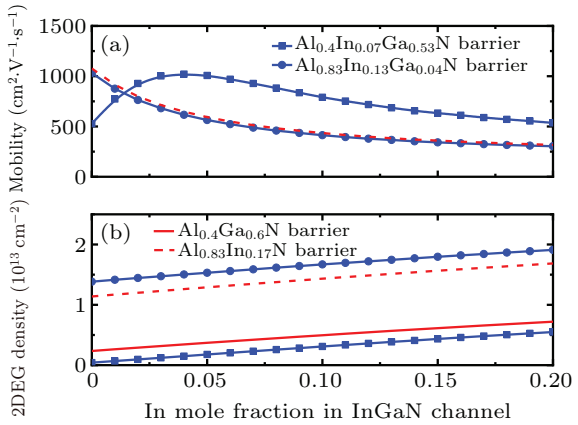


Fig. 5. Plots of electron mobility in Al(In)GaN/AlN/InGaN/GaN DH *versus* indium mole fraction in InGaN channel layer at room temperature.

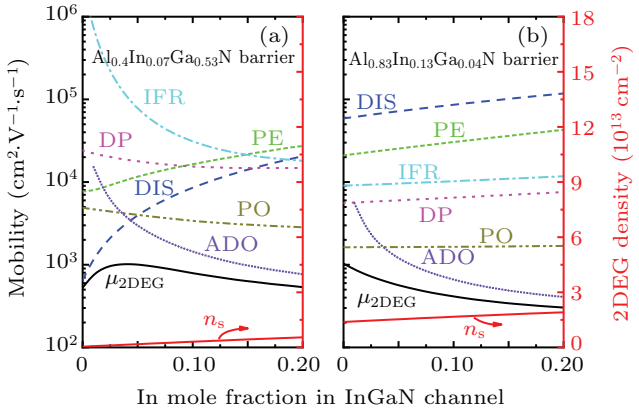


Fig. 6. Plots of electron mobility and 2DEG density *versus* indium mole fraction limited by various scattering mechanisms in InGaN channel layer at room temperature for (a) $Al_{0.4}In_{0.07}Ga_{0.53}N$/AlN/InGaN/GaN DH and (b) $Al_{0.83}In_{0.13}Ga_{0.04}N$/AlN/InGaN/GaN DH.

Finally, we investigate the temperature dependence of electron mobility in AlInGaN/AlN/$In_{0.04}Ga_{0.96}N$/GaN DHs with $Al_{0.4}In_{0.07}Ga_{0.53}N$ and $Al_{0.83}In_{0.13}Ga_{0.04}N$ barriers in Fig. 7, where 2DEG density is combined with the temperature-dependent band gaps. Although 2DEG density value is higher in $In_{0.04}Ga_{0.96}N$ channel-based DH with $Al_{0.83}In_{0.13}Ga_{0.04}N$ barrier than the case with $Al_{0.4}In_{0.07}Ga_{0.53}N$ barrier (on the order of 10^{13} cm^{-2} *versus* 10^{12} cm^{-2}), the increment of electron density in a temperature range from 10 K to 1000 K is relatively small in $Al_{0.83}In_{0.13}Ga_{0.04}N$/AlN/$In_{0.04}Ga_{0.96}N$/GaN DHs (9.6%), in contrast to the case with $Al_{0.4}In_{0.07}Ga_{0.53}N$ barrier (120.3%). Therefore, the temperature-independent scattering mechanisms, DIS, IFR, and ADO scatterings are changed by the noticeable variation of 2DEG density with temperature for the case with $Al_{0.4}In_{0.07}Ga_{0.53}N$ barrier but remain almost unchanged for the case with $Al_{0.83}In_{0.13}Ga_{0.04}N$ barrier. With the increase of temperature, the effects of several scattering processes related to lattice vibration, including PE scattering, DP scattering, and POP scattering are remarkably strengthened. Theoretically, mobility limited by DP or PE scattering is proportional to the reciprocal of temperature (μ_{DP}, $\mu_{PE} \propto T^{-1}$), while the influence of POP scattering increases exponentially as temperature rises ($\mu_{PO} \propto \exp(\hbar\omega_{LO}/k_BT)$, where $\hbar\omega_{LO}$ is the POP energy of InGaN channel, k_B is the Boltzmann constant), making POP scattering the main limiting scattering mechanism at temperature over 300 K in both cases. As shown in Fig. 7(a), 2DEG mobility is limited mainly by the DIS scattering for temperature below 320 K and then POP scattering for higher temperature in $Al_{0.4}In_{0.07}Ga_{0.53}N$/AlN/$In_{0.04}Ga_{0.96}N$/GaN DH, while for the case with $Al_{0.83}In_{0.13}Ga_{0.04}N$ barrier as shown in Fig. 7(b), the dominating scattering mechanism is ADO scattering for temperature below 310 K and POP scattering hereafter. Since the intensity of ADO scattering and POP scattering are both directly proportional to 2DEG density as shown in Fig. 4, higher density in InGaN channel-based DH with $Al_{0.83}In_{0.13}Ga_{0.04}N$ barrier results in lower mobility. As a result, the reduction of 2DEG mobility in a temperature range from 10 K to 1000 K is relatively small for the case with $Al_{0.4}In_{0.07}Ga_{0.53}N$ barrier (88.5%) compared to that for the case with $Al_{0.83}In_{0.13}Ga_{0.04}N$ barrier (92.2%).

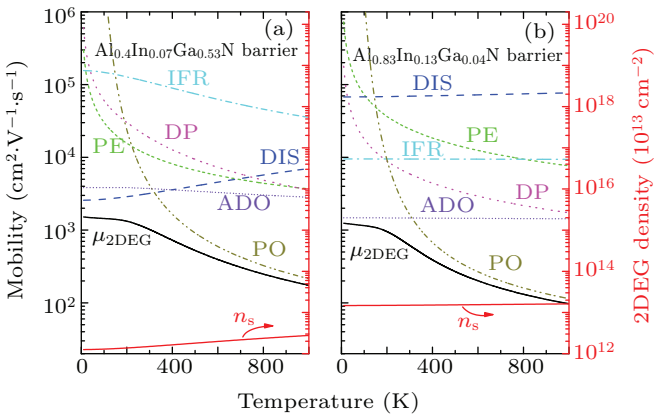


Fig. 7. The temperature-dependent electron mobility and the 2DEG density in (a) $Al_{0.4}In_{0.07}Ga_{0.53}N$/AlN/$In_{0.04}Ga_{0.96}N$/GaN DH, and (b) $Al_{0.83}In_{0.13}Ga_{0.04}N$/AlN/$In_{0.04}Ga_{0.96}N$/GaN DH.

3. Conclusions

In this paper, the electronic transport properties in AlInGaN/AlN/InGaN/GaN DH are analyzed based on a modified FH wave function and the effects of alloy composition from both barrier and channel layers are considered. The mobility in InGaN channel-based SH and InGaN channel-based DH behave as parabolic curves along the directions of increasing aluminum content and indium content of AlInGaN barrier,

while their corresponding 2DEG densities are apparently proportional to aluminum composition and inversely proportional to indium composition. For InGaN channel-based heterostructures with $Al_{0.4}Ga_{0.6}N$-like barrier layer, replacing few gallium with indium in barrier layer will reduce the mobility for InGaN channel with relatively small indium content (less than 0.35), but increases the mobility hereafter. While for the case with $Al_{0.83}In_{0.17}N$-like barrier layer, the substitution of indium for gallium brings minor effect on electron mobility. To achieve higher mobility, the optimal indium mole fraction in InGaN channel is 0.04 for the case with $Al_{0.4}In_{0.07}Ga_{0.53}N$ barrier, while for the $Al_{0.83}In_{0.13}Ga_{0.04}N$ barrier layer, the incorporation of indium depresses the mobility. Comparing with the case with $Al_{0.83}In_{0.13}Ga_{0.04}N$ barrier, the high temperature tolerance of mobility is slightly improved for $In_{0.04}Ga_{0.96}N$ channel-based DH with $Al_{0.4}In_{0.07}Ga_{0.53}N$ barrier layer.

References

[1] Hsin Y M, Hsu H T, Chuo C C and Chyi J I 2010 *IEEE Electron Dev. Lett.* **22** 501

[2] Chuo C C, Lee C M and Chyi J I 2001 *Appl. Phys. Lett.* **78** 314

[3] Wang C X, Tsubaki K, Kobayashi N and Makimoto T 2004 *Appl. Phys. Lett.* **84** 2313

[4] Sohi P, Carlin J F and Grandjean N 2018 *Appl. Phys. Lett.* **112** 262101

[5] Wang P Y, Zhang J F, Xue J S, Zhou Y B, Zhang J C and Hao Y 2011 *Acta Phys. Sin.* **60** 117304 (in Chinese)

[6] Li Y, Zhang J F, Wan W, Zhang Y C, Nie Y H, Zhang J C and Hao Y 2015 *Physica E* **67** 77

[7] Zhang Y C, Zhou X W, Xu S R, Zhang J F, Zhang J C and Hao Y 2016 *Appl. Phys. Express* **9** 061003

[8] Laboutin O, Cao Y, Johnson W, Wang R, Li G, Jena D and Xing H 2012 *Appl. Phys. Lett.* **100** 121909

[9] Wang R H, Li G W, Karbasian G, Guo J, Faria F, Hu Z Y, Yue Y Z, Verma J, Laboulin O and Cao Y 2013 *Appl. Phys. Express* **6** 016503

[10] Xie J, Leach J H, Ni X, Wu M, Shimada R, Özgür Ü and Morkoç H 2007 *Appl. Phys. Lett.* **91** 262102

[11] Li Y 2019 *Phys. Status Solidi B* **256** 1800704

[12] Cao Y 2015 *Electron. Lett.* **51** 1205

[13] Gökden S, Tülek R, Teke A, Leach J H, Fan Q, Xie J, Özgür Ü, Morkoç H, Lisesivdin S B and Özbay E 2010 *Semicond. Sci. Technol.* **25** 045024

[14] Kuzmík J 2002 *Semicond. Sci. Technol.* **17** 540

[15] Li Y, Zhang J F, Xue J S, Liu G P, R. D. Quan, Duan X L, Zhang J C and Hao Y 2018 *Phys. Status Solidi A* **215** 1700787